




Article

# Preparation and Properties of Plant-Oil-Based Epoxy Acrylate-Like Resins for UV-Curable Coatings

Jijun Tang <sup>1,†</sup>, Jinshuai Zhang <sup>2,†</sup>, Jianyu Lu <sup>1,2</sup>, Jia Huang <sup>2</sup>, Fei Zhang <sup>2</sup> , Yun Hu <sup>2</sup>, Chengguo Liu <sup>2,\*</sup> , Rongrong An <sup>3,\*</sup>, Hongcheng Miao <sup>2,4</sup>, Yuanyuan Chen <sup>2,4</sup>, Tian Huang <sup>2,4</sup> and Yonghong Zhou <sup>2,\*</sup> 

<sup>1</sup> College of Materials Science and Engineering, Jiangsu University of Science and Technology, Zhenjiang 212100, China; tangjijunnju@126.com (J.T.); oqqooo12@163.com (J.L.)

<sup>2</sup> Institute of Chemical Industry of Forest Products, Chinese Academy of Forestry, Nanjing 210042, China; zdslhs@126.com (J.Z.); hj18252588192@163.com (J.H.); zhangfei@jspi.cn (F.Z.); huyun@icifp.cn (Y.H.); mh460826041@163.com (H.M.); yuanyuanchen19@163.com (Y.C.); 1551kinoko@gmail.com (T.H.)

<sup>3</sup> College of Geographic and Biologic Information, Nanjing University of Posts and Telecommunications, Nanjing 210023, China

<sup>4</sup> College of Chemical Engineering, Nanjing Forestry University, Nanjing 210037, China

\* Correspondence: liuchengguo@icifp.cn (C.L.); anrongrong@njupt.edu.cn (R.A.); zyh@icifp.cn (Y.Z.); Tel./Fax: +86-25-85482520 (C.L.); +86-25-85866638 (R.A.); +86-25-854825777 (Y.Z.)

† These authors contributed equally to this work.

Received: 18 August 2020; Accepted: 9 September 2020; Published: 22 September 2020



**Abstract:** Novel oil-based epoxy acrylate (EA)-like prepolymers were synthesized via the ring-opening reaction of epoxidized plant oils with a new unsaturated carboxyl acid precursor (MAAMA) synthesized by reacting maleic anhydride (MA) with methallyl alcohol (MAA). Since the employed epoxidized oils including epoxidized soybean oil (ESO), epoxidized rubber seed oil (ERSO), and epoxidized wilsoniana seed oil (EWSO) possessed epoxy values of 7.34–4.38%, the obtained epoxy acrylate (EA)-like prepolymers (MMESO, MMERSO, and MMEWSO) indicated a C=C functionality of 7.81–4.40 per triglyceride. Furthermore, effects of the C=C functionality and the addition of hydroxyethyl methacrylate (HEMA) diluent on the ultimate properties of the resulting UV-cured EA-like materials were investigated and compared with those of commercially available acrylated ESO (AESO) resins. As the C=C functionality increased, the storage modulus at 25 °C ( $E'_{25}$ ), glass transition temperature ( $T_g$ ), 5% weight-loss temperature ( $T_5$ ), tensile strength and modulus ( $\sigma$  and  $E$ ), and hardness of the coating for both the pure EA and EA/HEMA resins increased significantly as well. These properties indicated similar trends when comparing the EA materials with 30% of HEMA with those pure EA materials. Specially, although ERSO had a clearly lower epoxy value than ESO, both the UV-cured pure MMERSO and MMERSO/HEMA materials showed much better  $E'_{25}$ ,  $T_g$ ,  $\sigma$ , and  $E$  than their AESO counterparts, indicating that the MAAMA modification of epoxidized plant oils was much more effective than the modification of acrylic acid to achieve high-performance oil-based epoxy acrylate resins.

**Keywords:** soybean oil; rubber seed oil; wilsoniana seed oil; epoxy acrylate; UV-curable coatings

## 1. Introduction

The ultraviolet (UV)-curing technique has received enormous interest in modern industrial areas such as coatings, inks, and adhesives due to its distinct advantages, including being efficient, energy-saving, enabling, economical, eco-friendly, etc. [1–6]. The global market of UV-curable resins was nearly \$3.1 billion in 2015 and is expected to reach \$4.6 billion in 2020, with an annual growth rate close to 8.7% for the period 2015–2020 [7]. However, most of the raw materials for UV-curable coatings currently

available in the global market are from non-renewable, environmentally polluting petroleum-based fossil resources. Therefore, developing UV-curable coatings by introducing biorenewable components such as carbohydrates, plant oils, and rosins related to sustainability and environmental protection is required to match sustainable development strategies [8,9].

Plant oils have the features of environmentally benign, abundance, biodegradability, and triglyceride structures; thus, they have been used as an ideal substitute to prepare bio-based prepolymers for UV-curable coatings [10–19]. Plant-oil-based epoxy acrylate (EA) is one of the common UV-curable prepolymers, which is usually prepared through the ring-opening reaction of epoxidized plant oils with acrylic acid (AA) or its derivatives. Acrylated epoxidized soybean oil (AESO), perhaps the most often bio-based UV-curable prepolymer, has been proverbially employed in the fields of coatings and adhesives [7,15,20–22]. However, most of the reported oil-based EA resins usually possessed low stiffness and heat resistance, which greatly limited their application in the areas where petroleum-based EA resins can be used. For example, the tensile modulus and  $T_g$  of bisphenol A epoxy acrylate resin reported by Xiao et al. could reach 300–500 MPa and 75 °C, respectively, while the pure AESO resin only showed a tensile modulus of around 60 MPa and  $T_g$  of about 20 °C due to its lack of rigid structure [23,24]. Therefore, a variety of works dedicated to improving such properties for oil-based EA resins have been conducted [7,20–22,25–29], among which the design of new oil-based EA prepolymers has gained much attention. For instance, Li et al. [22] synthesized a novel EA prepolymer from soybean oil (SO) through melt ring-opening reaction of epoxidized soybean oil (ESO) with monomethyl itaconate. However, the resulting monomethyl itaconated epoxidized soybean oil (IESO) materials generally exhibited no clear improvement in strength, stiffness, and heat resistance in comparison with the AESO counterparts, which is probably attributed to that the C=C functionality of IESO (2.39 per ESO) being similar to that of AESO (2.25 per ESO). In our group, we also developed a novel SO-based EA prepolymer through the modification of ESO with an unsaturated carboxylic acid precursor (HEMAMA) prepared by reacting hydroxyethyl methacrylate (HEMA) with maleic anhydride (MA) [30]. Due to the precursor having two active C=C groups and a side methyl group, the resultant SO-based EA prepolymers possessed both high functionality (5.51–6.05 per ESO) and the structure of steric hindrance. Therefore, the properties such as tensile strength and modulus, storage modulus at 25 °C,  $T_g$ , and pencil hardness for the UV-cured EA materials were all greatly improved compared with the AESO material. However, up until now, novel oil-based EA resins with high performance are still very scarce, and whether the important properties can be tuned by varying the renewable raw materials such as epoxidized plant oils are unknown.

Soybean oil, with a global production that amounted to 56.52 million tons in 2019/2020, has become a very attractive bio-based alternative to petroleum-based compounds in polymeric materials [10]. In addition, some woody plant oils such as rubber seed oil (RSO) and *wilsoniana* seed oil (WSO) also make up a great proportion of the current consumption of bio-based feedstocks in the chemical industries as they do not compete with agricultural food production [31–33]. In 2013, the global total production of natural rubber latex was estimated to reach 11.9 million tons, and this figure is expected to increase significantly with the further expansion of planting areas [34]. *Wilsoniana* tree is also a widely distributed woody oil plant in the south of China, and the annual production of WSO could reach 30 million tons [33]. The RSO and WSO have been used in the areas of coatings [35–37], plasticizers [38], and some other fields [33,39]. Nevertheless, up to now, their employment in the construction of UV-curable coatings has not been reported yet.

In this paper, we aim to develop high-performance oil-based EA resins using epoxidized plant oils with different epoxy values. According to the above analysis, incorporating high functionality and the structure of steric hindrance into the new EA prepolymers is an effective way to fulfill the purpose. Therefore, a new unsaturated carboxyl acid precursor (MAAMA), obtained through the reaction of methallyl alcohol (MAA) with maleic anhydride (MA), was used to modify epoxidized plant oils including ESO, epoxidized RSO (ERSO), and epoxidized WSO (EWSO). It should be noted that the employed epoxidized plant oils possessed a decreasing epoxy value from 7.34% to 4.38%,

thus resulting in the corresponding EA-like prepolymers with an introduced C=C functionality of 7.81 to 4.40 per triglyceride. In addition, the effects of C=C functionality and incorporating HEMA diluent on the physiochemical properties and UV-curing behaviors of the resultant oil-based EA resins were investigated and compared with commercial AESO resins.

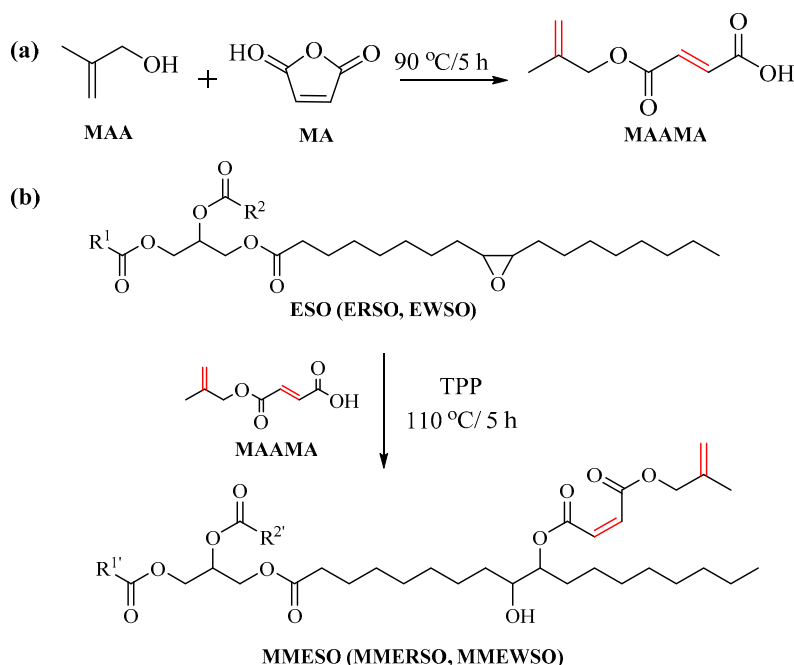
## 2. Experimental

### 2.1. Materials

ESO was obtained from Shanghai Aladdin Chemistry Co., Ltd. (Shanghai, China), and possessed an epoxy value of 7.34%. RSO and WSO were provided by Southwest Forestry University (Yunnan, China). AESO with a viscosity of 37,500 mPa s, was supplied by Shandong Shouguang Luke Chemical Co., Ltd. (Shandong, China). The methallyl alcohol (MAA, 98%) and hydroxyethyl methacrylate (HEMA,  $\geq 97\%$ ) were provided by Macklin Chemical Reagent Co., Ltd. (Shanghai, China). Maleic anhydride (MA,  $\geq 99.5\%$ ) was provided by Nanjing Chemical Co., Ltd. (Nanjing, China). Triphenylphosphine (TPP,  $\geq 98\%$ ) was supplied by Sinopharm Chemical Reagent Co., Ltd. (Shanghai, China). 4-Methoxyphenol (MEHQ,  $\geq 99\%$ ) was supplied by Shanghai Titan Technology Co., Ltd. (Shanghai, China). Darocur 1173 (98%) was provided by Saen Chemical Technology Co., Ltd. (Zhengzhou, China).

### 2.2. Synthesis of MAAMA

About 28.5 g of MAA, 39.2 g of MA, and 0.136 g of MEHQ were mixed into a 250 mL four-neck round-bottom flask fitted with a mechanical stirrer, thermometer, refluxing condenser, and a nitrogen inlet. Then, the reaction was performed at 70 °C under the protection of N<sub>2</sub> until solidified MA completely melted. Subsequently, the mixture was heated to 90 °C for 5 h, and a golden yellow transparent liquid at room temperature was obtained (see Scheme 1 for synthesis route).



**Scheme 1.** Synthesis route for new unsaturated carboxyl acid precursors obtained through the reaction of (a) methallyl alcohol (MAA) with maleic anhydride (MAA) (MAAMA) and (b) obtained epoxy acrylate-like prepolymers MMESO, MMERSO, and MMEWSO. ESO: epoxidized soybean oil, ERSO: epoxidized rubber seed oil, EWSO: epoxidized wilsoniana seed oil.

### 2.3. Epoxidation of Plant Oils

ERSO was synthesized as follows: approximately 42.7 g of RSO, 4.5 g of formic acid, and 50 mL of toluene were mixed in a four-necked round-bottom flask. Subsequently, about 3.0 g of concentrated sulfuric acid and 51 g of 30% hydrogen peroxide were added dropwise into the flask under 50 °C within 30 min. After that, the mixture was heated to 70 °C for 5 h. Finally, the product was washed by distilled water until neutral, and then a pale yellow transparent liquid that possessed an epoxy value of 5.15% was obtained. EWSO was synthesized in the same way, and its epoxy value was 4.38%.

### 2.4. Synthesis of MMESO, MMERSO, and MMEWSO

The synthesis methods of MMESO, MMERSO, and MMEWSO are similar, taking the synthesis of MMESO as an example (Scheme 1). Typically, 50 g of ESO, 35.83 g of MAAMA, 0.086 g of MEHQ, and 0.86 g of TPP were charged into a four-neck round-bottom flask. Under the protection of N<sub>2</sub>, the mixture was agitated under 110 °C for 2 h. During the work-up procedures, the resulting crude MMESO product was washed by 10 wt % NaCl/H<sub>2</sub>O solutions three times, dissolved by dichloromethane, dried with MgSO<sub>4</sub>, and evaporated via rotary evaporation. Finally, a light-yellow, viscous liquid product at room temperature was obtained.

### 2.5. Curing of MMESO, MMERSO, and MMEWSO Resins

The UV-curable resins were obtained by mixing pure EA-like prepolymers (MMESO, MMERSO, or MMEWSO), HEMA, and Darocur 1173 photoinitiator at room temperature. The formulations of EA or EA/HEMA resins are shown in Table 1. Take the synthesis of MMESO/HEMA30 as an example: about 7.0 g of MMESO, 3 g of HEMA, and 0.15 g of Darocur 1173 were mixed in a round-bottom flask fitted with a mechanical stirrer. Then, the mixture was agitated at room temperature for about 30 min, followed by degassing under vacuum for about 10 min. Then, the resulting samples were cast into a self-made polytetrafluoroethylene mold or coated on polished tinfoil sheets by a filmmaker. Finally, the casted or coated samples were cured by an Intelli-Ray 400W UV light-curing microprocessor with a UV wavelength of 320–390 nm from Uvitron International Corporation (USA). The exposure intensity and time for all the samples were 100 mW/cm<sup>2</sup> and 20 min, respectively.

**Table 1.** Composition of UV-cured epoxy acrylate (EA)-like samples. HEMA: hydroxyethyl methacrylate.

Samples *	EA (wt %)	HEMA (wt %)	Darocur 1173 (wt %)
MMESO	100	0	1.5
MMERSO	100	0	1.5
MMEWSO	100	0	1.5
MMESO/HEMA30	70	30	1.5
MMERSO/HEMA30	70	30	1.5
MMEWSO/HEMA30	70	30	1.5

\* The epoxy values of ESO, ERSO, and EWSO used for the synthesis of EA-like prepolymers were 7.34%, 5.15%, and 4.38%, respectively.

### 2.6. Characterization

#### 2.6.1. Acid Value (*A<sub>v</sub>*)

Acid values of samples were determined based on the procedures outlined in GB/T 2895-1982, as provided in a previous work of us [40].

#### 2.6.2. Epoxy Values (*E*)

Epoxy values were recorded based on the procedures outlined in GB 1677-81. Approximately 0.5 g of the sample was completely dissolved in 20 mL of chlorhydric acid/acetone solution; then,

bromocresol was added as an indicator. Finally, the solution was titrated by 0.15 mol/L NaOH solution. The epoxy value (g/100g) of the sample was determined using the following equation:

$$E = \frac{(V_1 - V_2) \times C_{\text{NaOH}} \times 16}{10m} \quad (1)$$

where  $V_1$  = blank burette reading (mL),  $V_2$  = sample burette reading (mL),  $C_{\text{NaOH}}$  = initial concentration of NaOH solution, 16 = molar mass of oxygen atom,  $m$  = weight of sample (g).

#### 2.6.3. Fourier Transform Infrared Spectroscopy Analysis (FT-IR)

FT-IR tests were conducted on a Nicolet iS10 IR spectrometer from Thermo-Fisher Corporation (Thermo-Fisher Corporation, Waltham, Massachusetts, USA) within a scanning range from 650 to 4000  $\text{cm}^{-1}$ .

#### 2.6.4. Nuclear Magnetic Resonance Analysis (NMR)

$^1\text{H}$  NMR tests were conducted on a DRX-300 Advance NMR spectrometer from Bruker Corporation (Bruker Corporation, Karlsruhe, Germany) with  $\text{CDCl}_3$  as a solvent.

#### 2.6.5. Gel Content ( $C_{\text{gel}}$ )

The  $C_{\text{gel}}$  tests of MMEVO samples were performed via Soxhlet extraction. Typically, approximately 0.5 g of the cured samples were precisely weighed (recorded as  $m_0$ ), extracted by acetone for 24 h, and finally dried at 60 °C until a constant mass was obtained (recorded as  $m_1$ ). The  $C_{\text{gel}}$  values of samples were calculated as  $m_1/m_0$  [41].

#### 2.6.6. Dynamic Mechanical Analysis (DMA)

The DMA test of the samples was carried out on a Q800 solids analyzer (TA Corporation, New Castle, PA, USA) under the conditions including a stretching mode, a frequency of 1 Hz, a temperature within a range of −50 to 200 °C, and a heating rate of 3 °C/min. The size of the tested samples was about 40 × 6 × 1  $\text{mm}^3$ .

#### 2.6.7. Thermogravimetric Analysis (TGA)

The TGA test of the samples was performed using an STA 409PC thermogravimetry instrument from Netzsch Corporation (Netzsch Corporation, Bavaria, Germany) under  $\text{N}_2$  at a flow rate of 100 mL/min. The cured samples were ground to powders before the test. About 10 mg of the powder for each sample was tested in a temperature range of 40 to 600 °C and at a heating rate of 15 °C/min.

#### 2.6.8. Mechanical Properties

The tensile properties of samples were analyzed using a UTM 4304 universal tester (Shenzhen Suns Technology Corporation, Shenzhen, China) with a speed of 5 mm/min. Five specimens with a size of 80 × 10 × 1  $\text{mm}^3$  were evaluated for each sample to calculate the average values.

#### 2.6.9. Coating Properties

Adhesion of the UV-cured coatings was evaluated by an adhesion test machine (Tianjin Shiboweiye Glass Instrument Corporation, Tianjin, China) according to the procedures specified in GB 1720-79(89). The adhesion grade ranged from 1 to 7 grade (1 grade is the best). The pencil hardness of the UV-cured coatings was measured on a QHQ-A pencil hardness tester from Tianjin Litengda Instrument Corporation based on the procedures listed in GB/T 6739-2006. The pencil hardness mainly includes 6H to H, HB, and B to 6B (from the hardest to the softest). Flexibility of the UV-cured coatings was tested by a QTY-32 paint film cylindrical bending machine from Tianjin Litengda Instrument Corporation (China) according to the procedures listed in GB/T 1731-93. The class of flexibility involves 2, 3, 4, 6, 8,

10, 12, 14 mm, etc., (2 mm is the best). Detailed procedures for the coating tests were indicated in a previous work of ours [30,42].

### 2.6.10. UV-Curing Kinetics

The UV curing behaviors of the obtained liquid resins were tested by a modified Nicolet 5700 spectrometer (Thermo-Nicolet Instrument Corporation, Madison, WI, USA). The C=C conversion rate ( $\alpha_{C=C}$ ) was recorded by monitoring the absorption intensity of the C=C peak at approximately  $810\text{ cm}^{-1}$ , which can be calculated using the following equation [43,44]

$$\alpha_{C=C} = \frac{A_0 - A_t}{A_0} \times 100\% \quad (2)$$

where  $A_0$  and  $A_t$  are the C=C peak areas at the original time and  $t$  time, respectively.

## 3. Results and Discussion

### 3.1. Synthesis and Characterization of Oil-Based EA-Like Prepolymers

The synthesis of pure EA-like prepolymers mainly involved two steps, as displayed in Scheme 1.  $A_v$  values of the products were used to monitor the reaction extents. First, the synthesis process of the MAAMA precursor was investigated, as shown in Figure S1. After being performed at  $90\text{ }^\circ\text{C}$  for 5 h, its  $A_v$  value was basically stable at around  $329.8\text{ mgKOH/g}$ , which was very close to the theoretical acid value of  $332.1\text{ mgKOH/g}$ . Second, MAAMA was used to modify ESO, ERSO, and EWSO, and after being reacted at  $90\text{ }^\circ\text{C}$  for 2 h, the  $A_v$  values of the reaction mixtures were all below  $25\text{ mgKOH/g}$  (as shown in Table 2). Finally, the corresponding EA-like precursors (MMESO, MMERSO, and MMEWSO) products were obtained.

**Table 2.** Properties of UV-cured EA-like samples. AESO: acrylated ESO.

Samples	$A_v$ <sup>a</sup> mgKOH/g	$N_{C=C}$ <sup>b</sup>	$C_{\text{bio}}$ <sup>c</sup> (%)	$C_{\text{gel}}$ <sup>d</sup> (%)
AESO	18.2	2.25	84.1	93.1
MMESO	20.2	7.81	59.0	95.9
MMERSO	23.2	5.92	65.1	93.3
MMEWSO	22.4	4.40	71.3	87.1
AESO/HEMA30	-	-	58.8	98.0
MMESO/HEMA30	-	-	41.3	99.9
MMERSO/HEMA30	-	-	45.6	99.5
MMEWSO/HEMA30	-	-	50.0	98.5

<sup>a</sup> Acid value. <sup>b</sup> Introduced C=C functionality per triglyceride. <sup>c</sup> Bio-based. content. <sup>d</sup> Gel content.

Chemical structures of the MAAMA, ESO, and final EA-like prepolymers MMESO were characterized by FT-IR, as depicted in Figure 1. The FT-IR spectra of ERSO, MMERSO, EWSO, and MMEWSO are depicted in Figure S2. In the MAAMA spectrum, the strong absorption bands around  $2500\text{--}3400\text{ cm}^{-1}$ ,  $1643\text{ cm}^{-1}$ , and  $816\text{ cm}^{-1}$  were attributed to the characteristic peaks of carboxyl groups, C=C extensional vibration, and C=C bend vibration, respectively [45]. In the spectra of ESO, ERSO, and EWSO, the peaks at  $823\text{ cm}^{-1}$  related to epoxy groups were observed [23]. As for the spectra of MMESO, MMERSO, and MMEWSO, the epoxy peak at  $823\text{ cm}^{-1}$  and the carboxyl peak at  $2500\text{--}3400\text{ cm}^{-1}$  basically disappeared, while a new small peak at around  $3540\text{ cm}^{-1}$  assigned to the hydroxyl group appeared [22,46,47]. These changes indicated that the epoxy groups on epoxidized plant oils (EPO) successfully reacted with the carboxyl group on MAAMA. Besides, new peaks at  $816$  and  $1643\text{ cm}^{-1}$  appeared, which could be assigned to the C=C bend vibration and C=C stretching vibration, respectively. All these changes indicated that EPO has been successfully grafted by MAAMA.

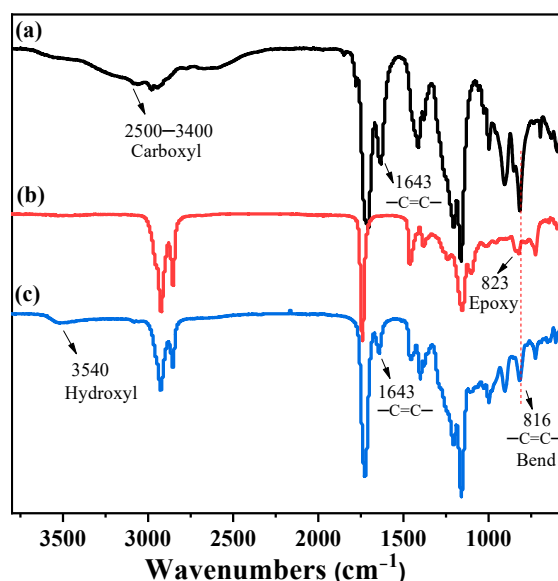


Figure 1. FT-IR spectra of (a) MAAMA, (b) ESO, and (c) MMESO.

The  $^1\text{H}$  NMR spectra of MAAMA, ESO, and MMESO are presented in Figure 2. The  $^1\text{H}$  NMR spectra of ERSO, MMERSO, EWSO, and MMEWSO are depicted in Figure S3. In the spectrum of MAAMA, the peak at 11.9 ppm corresponds to the protons of carboxyl groups due to the ring-opening reaction of MA [30]. The peaks at 4.94 and 6.37 ppm could be assigned to the C=C protons on methallyl ester and maleate, respectively [4]. The peaks at 1.73 ppm were assigned to the three-terminal methyl protons in methallyl alcohol, which are always used as a reference since its intensity should not alter during the modification. According to Figure S4, the C=C functionality of MAAMA can be calculated from the peaks at 4.8–5.1 ppm and 6.0–6.9 ppm and it was 1.98, which was very close to the theoretical value of 2. In the spectra of ESO, ERSO, and EWSO (Figure 2 and Figure S3), the peaks at 2.8–3.2 ppm correspond to the protons on epoxy groups [48]. The peaks at around 0.88 ppm were assigned to the terminal methyl protons in triglycerides, which can be used as a reference to estimate the amount of epoxy group, since it is inactive throughout the modification process. Based on Figures S5–S7, the introduced oxirane groups per triglyceride of ESO, ERSO, and EWSO were 4.36, 3.0, and 2.53, respectively. In the spectra of MMESO, MMERSO, and MMEWSO (Figure 2 and Figure S3), the peaks at 11.9 ppm and 2.8–3.2 ppm respectively corresponding to the carboxyl groups and the epoxy group almost disappeared, indicating the reaction between them. Meanwhile, a new peak at about 4.0 ppm attributed to the methine protons on the connecting structure of MAAMA and ESO, ERSO, and EWSO occurred [30]. Besides, new strong peaks at around 4.8–5.1 ppm and 6.0–6.9 ppm appeared, which can be ascribed to the introduced C=C protons from MAAMA. The introduced C=C functionality on the EA-like prepolymers could also be calculated according to the reference peak at 0.88 ppm. Based on Equation (3) and Figures S8–S10, the introduced C=C functionality for ESO, ERSO, and EWSO was 7.81, 5.92, and 4.40, respectively, which was much higher compared to the commercial AESO products (2.25, see Equation (S1) and Figure S11) [40].

$$N_{\text{C}=\text{C}} = \frac{(A_{4.8-5.1 \text{ ppm}} + A_{6.0-6.9 \text{ ppm}})/2}{A_{0.88 \text{ ppm}}/9} = \frac{9(A_{4.8-5.1 \text{ ppm}} + A_{6.0-6.9 \text{ ppm}})}{2A_{0.88 \text{ ppm}}} \quad (3)$$

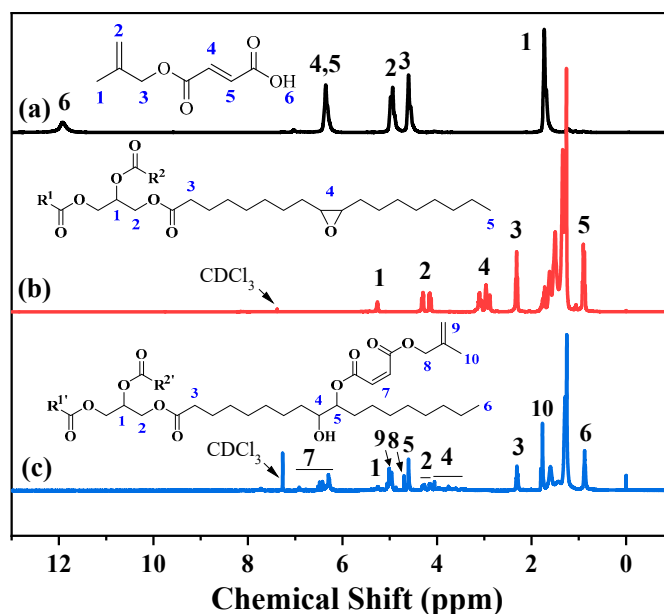


Figure 2.  $^1\text{H}$  NMR spectra of (a) MAAMA, (b) ESO, and (c) MMESO.

In theory, the  $\text{C}=\text{C}$  functionality introduced ( $N_{\text{C}=\text{C}}$ ) in MMESO, MMERSO, and MMEWSO should be twice the amount of epoxy groups consumed ( $C_{\text{epoxy}}$ ) in ESO, ERSO, and EWSO, respectively. In reality, the  $\text{C}=\text{C}$  functionality introduced was slightly less than twice the oxirane group consumption. This may be due to the incomplete reaction or side reactions that occurred during EA synthesis. For instance, it could allow an oligomerization between oxirane and oxirane groups caused by the residual MAA or MA [26,30,49].

### 3.2. Bio-Based Content of the UV-Cured EA-Like Materials

The bio-based content of a material can be defined as the amount of bio-based carbon as a percentage of the total organic carbon weight in the product [2,42,47]. According to this definition, the bio-based contents of the neat ESO, ERSO, EWSO, MAAMA, HEMA, HEA, and Darocur 1173 were 100%, 100%, 100%, 0%, 0%, 0%, and 0%, respectively. The bio-based contents of the resulting materials are listed in Table 2. As the  $\text{C}=\text{C}$  functionality increased, the bio-based content of the UV-cured pure EA resins decreased gradually. Since the pure MMESO material possessed the highest  $\text{C}=\text{C}$  functionality, it presented the lowest bio-based carbon content of 59.0%. In contrast, AESO contained the lowest  $\text{C}=\text{C}$  functionality and therefore exhibited the highest content up to 84.1%. Similar trends were observed for the EA/HEMA materials. In addition, a significant decrease in the bio-based content of EA-like resin was observed when incorporating 30% of HEMA diluent. For instance, the bio-based content of MMESO/HEMA30 dropped from 59.0% in pure MMESO to 41.3%.

### 3.3. Gel Contents of the UV-Cured EA-Like Materials

Gel content ( $C_{\text{gel}}$ ) is closely related to the final properties of thermosetting materials because it can reflect the cross-link extent of the thermosets [2]. The  $C_{\text{gel}}$  values of the UV-cured EA or EA/HEMA materials are displayed in Table 2. The UV-cured pure MMESO and MMERSO materials demonstrated a higher  $C_{\text{gel}}$  than commercially available AESO resins, suggesting that they had a higher cross-link extent than AESO. Similar trends were observed when comparing the three EA/HEMA30 materials with the AESO/HEMA30 materials. As the  $\text{C}=\text{C}$  functionality on EPO rose from 4.40 to 7.81, the  $C_{\text{gel}}$  values of the pure EA materials increased from 87.1% to 95.9%, and the values of the EA/HEMA materials increased from 98.5% to 99.9%. These results indicated that the improved functionality of thermosets can effectively enhance the cross-link extent of the resulting UV-cured materials. Furthermore, the  $C_{\text{gel}}$  values of the cured EA/HEMA resins containing 30% of HEMA diluent were apparently improved



compared to those of pure EA resin, which demonstrated that the incorporation of diluent was beneficial to the improvement of the cross-linking of the UV-cured materials.

### 3.4. Properties of the UV-Cured EA-Like Materials

#### 3.4.1. Dynamic Mechanical Analysis

The dynamic mechanical analysis including the storage modulus ( $E'$ ) and loss factor ( $\tan \delta$ ) of the UV-cured EA-like samples is demonstrated in Figure 3, and the related data are summarized in Table 3. The glass transition temperature ( $T_g$ ) was defined as the peak temperature of  $\tan \delta$  curves, and the cross-link density ( $\nu_e$ ) of the cured resins was calculated using the following equation [2,22,50]

$$\nu_e = \frac{E'}{3RT} \quad (4)$$

where  $E'$  is the storage modulus of the resins in the rubber state (the  $E'$  at  $T_g + 60$  °C was selected to calculate  $\nu_e$  in this work),  $R$  represents the gas constant, and  $T$  represents the absolute temperature. Firstly, the pure MMESO material showed the  $E'$  at 25 °C ( $E'_{25}$ ) values of 697.5 MPa and  $T_g$  values of 69.4 °C, which were 7.0 and 4.4 times the values of the neat AESO material, respectively. The pure MMERSO material also showed much better  $E'_{25}$  and  $T_g$  than the pure AESO material, although ERSO had a clearly lower epoxy value than ESO. Similar results were demonstrated when comparing the MMESO/HEMA30 and MMERSO/HEMA30 materials with the AESO/HEMA30 material. All the results indicated that the MAAMA modification of epoxidized plant oils was much more effective to achieve high-performance plant oil-based EA resins than the common acrylic acid (AA) modification. Secondly, for the UV-cured pure EA materials, as the C=C functionality increased, the  $E'_{25}$  improved from 42.6 to 697.5 MPa,  $T_g$  improved from 17.2 to 69.4 °C, and  $\nu_e$  increased from  $0.86 \times 10^3$  to  $5.74 \times 10^3$  mol/m<sup>3</sup>. The improvement of  $E'_{25}$  and  $T_g$  probably results from the increase of  $\nu_e$  and the incorporation of more methyl steric structure from MAA. Similar trends were observed for the EA/HEMA materials, except that the MMEWSO/HEMA30 system demonstrated two  $T_g$  values, which indicated the existence of phase separation. For instance, the MMESO/HEMA30 material showed a  $T_g$  value of 84.0 °C, which was clearly higher than that of bisphenol A epoxy acrylate resin [24]. In addition, compared to the pure EA systems, the  $E'_{25}$  and  $T_g$  values of the EA/HEMA materials increased significantly, while the  $\nu_e$  values decreased during this change. The decline of  $\nu_e$  values probably lies in that the added diluent is a monofunctional monomer, which increased the effective molecular weight between cross-linked sites [41]. Therefore, the growth of  $E'_{25}$  and  $T_g$  values can be ascribed to the methyl steric hindrance from HEMA [22,41]. These results also suggested that the steric structure of HEMA played a more crucial part than the  $\nu_e$  values in determining the thermal–mechanical properties of the novel EA-like materials.

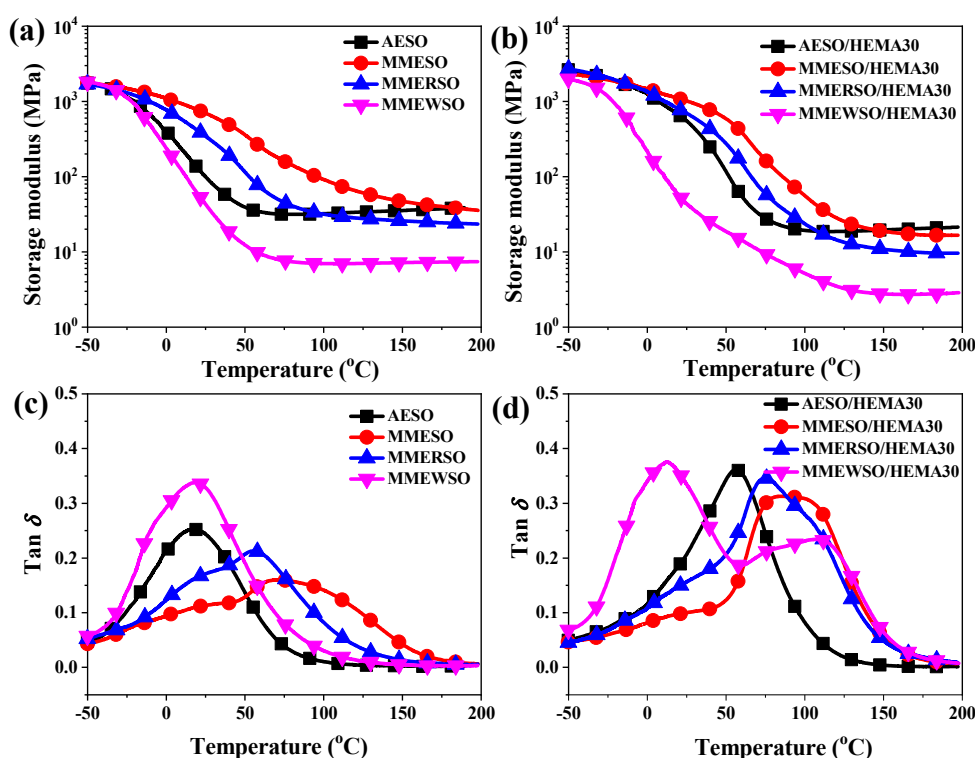


Figure 3. Storage modulus (a,b) and loss factor(c,d) of the UV-cured EA-like materials.

Table 3. Dynamic Mechanical Analysis (DMA) and Thermogravimetric Analysis (TGA) results of the UV-cured EA-like materials.

Samples	$E'_{25}$ <sup>a</sup> (MPa)	$T_g$ <sup>b</sup> (°C)	$E'_{T_g+60}$ <sup>c</sup> (MPa)	$\nu_e$ <sup>d</sup> ( $\times 10^3$ mol/m <sup>3</sup> )	$T_5$ <sup>e</sup> (°C)	$T_p$ <sup>f</sup> (°C)	$W_{char}$ <sup>g</sup> (%)
AESO	99.2	15.7	31.6	3.63	331.2	401.0	1.54
MMESO	697.5	69.4	57.6	5.74	271.1	399.8	3.01
MMERSO	343.5	55.6	28.8	2.97	265.9	401.6	1.96
MMEWSO	42.6	17.2	7.5	0.86	251.0	399.8	3.08
AESO/HEMA30	550.9	56.2	18.6	1.91	292.2	432.2	2.14
MMESO/HEMA30	1017.2	84.0	19.8	1.92	281.3	426.3	3.37
MMERSO/HEMA30	695.7	73.9	12.2	1.20	271.4	411.3	4.09
MMEWSO/HEMA30	43.7	17.5, 107.8	2.7	0.25	263.8	408.9	4.05

<sup>a</sup> Storage modulus at 25 °C. <sup>b</sup> Glass transition temperature, for MMEWSO/HEMA30 system, the second ones were employed to calculate cross-link density. <sup>c</sup> Storage modulus at  $T_g + 60$  °C. <sup>d</sup> Cross-link density. <sup>e</sup> 5% Thermal weight loss temperature. <sup>f</sup> Peak temperature at the curves of the weight-loss rate. <sup>g</sup> Char yield.

### 3.4.2. Thermogravimetric Analysis

TGA analysis of the UV-cured EA-like materials is depicted in Figure 4 and the corresponding data involving 5% weight-loss temperature ( $T_5$ ), the peak temperature of the weight-loss rate curves ( $T_p$ ), and char yield ( $W_{char}$ ) are summarized in Table 3. Firstly, the  $T_5$  values for the pure EA and EA/HEMA materials were clearly lower than those of the AESO counterparts. This is because the EA prepolymers contained more ester groups than AESO, which is detrimental to the initial thermal stability of the resulting polymeric materials [2,44]. Differently, the  $T_p$  values of the pure EA materials were almost the same as those of the pure AESO material, while the  $T_p$  values of the EA/HEMA materials were lower than those of the AESO/HEMA material. The decline of  $T_p$  probably results from that the EA/HEMA materials showed a larger drop of  $\nu_e$  than the AESO/HEMA material when incorporating HEMA into the materials. Secondly, for the pure EA materials, as the C=C functionality increased, the  $T_5$  values increased from 251.0 to 271.1 °C, while the  $T_p$  values fluctuated at about 400 °C. However, for the EA/HEMA materials, both  $T_5$  and  $T_p$  values increased clearly with the increase of C=C functionality. The rise of  $T_5$  and  $T_p$  values is probably ascribed to the growth of  $\nu_e$  for both the

pure EA and EA/HEMA systems. In addition, the obtained EA/HEMA materials showed better  $T_5$  and  $T_p$  values than the neat EA materials, indicating that the incorporation of HEMA diluent had a positive effect on the thermal stability of the EPO-based materials.

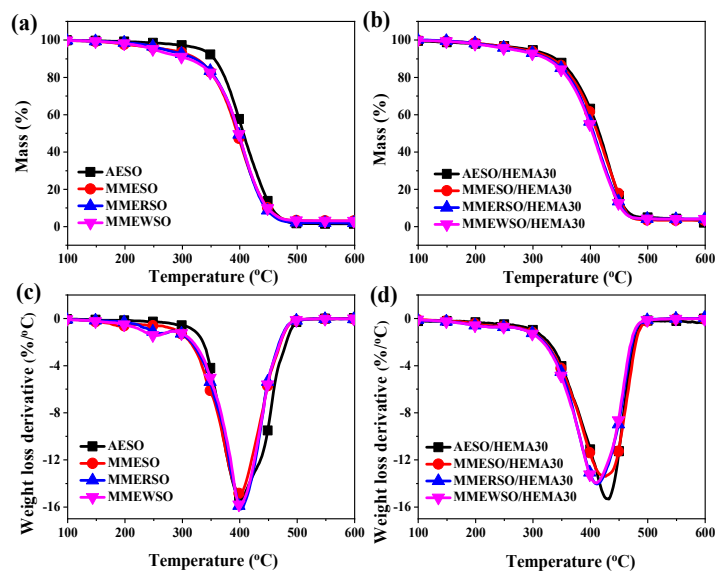


**Figure 4.** TGA curves (a,b) and their derivatives (c,d) of the UV-cured EA-like materials.

### 3.4.3. Mechanical Properties

Figure 5 exhibited the typical stress–strain curves of the resulting EA-like materials, and the related data are listed in Table 4. Notably, the neat MMESO material exhibited tensile strength and modulus ( $\sigma$  and  $E$ ) of 9.42 MPa and 200.3 MPa, respectively, which was 9.2 and 3.4 times the neat AESO resin. The neat MMERSO material also indicated much better tensile  $\sigma$  and  $E$  than the neat AESO material, although ERSO had an obviously lower epoxy value than ESO. Similar results were discovered in the cured EA materials with HEMA diluent. These results also demonstrated that the MAAMA modification of epoxidized plant oils was much more effective than the AA modification for high-performance oil-based epoxy acrylate resins, which agreed very well with the DMA results mentioned above. For the pure EA materials, as the C=C functionality increased,  $\sigma$  improved from 1.17 to 9.42 MPa,  $E$  improved from 19.4 to 200.3 MPa, and breaking strain ( $\epsilon$ ) decreased from 6.26% to 2.49%, respectively. Similar trends were demonstrated for the EA/HEMA materials. These variations can be attributed to the increase of cross-link density. As we know, an increase in cross-link density usually results in the improvement of stiffness and decrease of flexibility and toughness, and vice versa [30,51]. In addition, as the HEMA diluent content increased from 0 to 30%, the values of  $\sigma$ ,  $E$ , and  $\epsilon$  improved remarkably. For instance, the cured MMESO/HEMA30 material exhibited a  $\sigma$  value of 15.81 MPa and  $E$  value of 259.2 MPa, which were comparable to the similar ESO-based UV-curable coatings [7]. The obtained MMERSO/HEMA30 possessed a  $\sigma$  value of 10.12 MPa,  $E$  value of 186.7 MPa, and  $\epsilon$  value of 14.56, which were 3.5, 2.4, and 2.6 times the values of the pure MMERSO material, respectively. These results meant that the addition of HEMA diluent not only enhanced the rigidity of the resin but also improved the flexibility and toughness of resins. The reason for these changes lies in that the incorporation of HEMA could introduce methyl steric hindrance in the resulting bio-based materials, which was in good accordance with the DMA results, too.

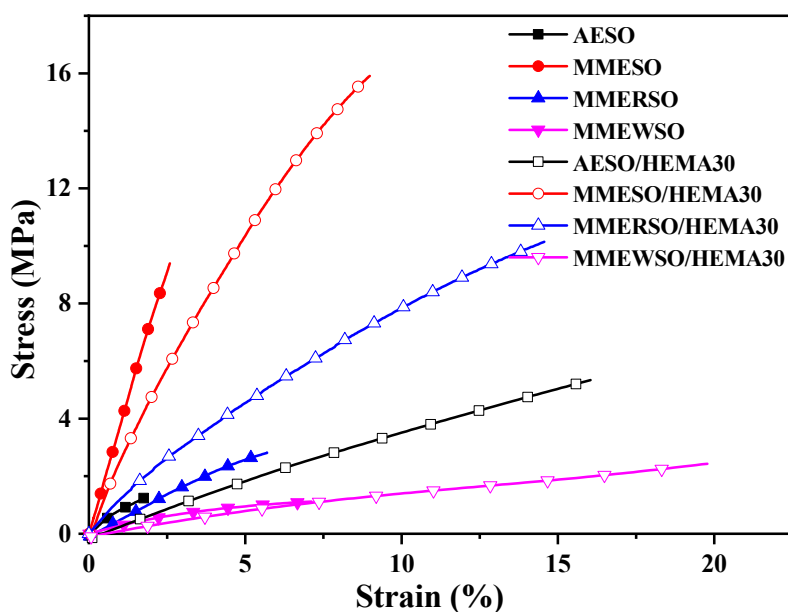


Figure 5. Stress–strain curves of the UV-cured EA-like materials.

Table 4. Mechanical properties and coating performance of the UV-cured EA-like materials.

Samples	$\sigma^a$ (MPa)	$E^b$ (MPa)	$\varepsilon^c$ (%)	Ad. <sup>d</sup> (Grade)	P.H. <sup>e</sup>	Fl <sup>f</sup> (mm)
AESO	1.02 ± 0.17	59.5 ± 8.2	1.75 ± 0.91	4	6B	2
MMESO	9.42 ± 0.79	200.3 ± 29.0	2.49 ± 0.86	3	5B	2
MMERSO	2.90 ± 0.32	76.6 ± 5.4	5.55 ± 0.79	4	6B	2
MMEWSO	1.17 ± 0.26	19.4 ± 2.4	6.26 ± 1.33	4	6B	2
AESO/HEMA30	5.30 ± 0.12	83.3 ± 5.0	15.61 ± 0.56	2	2H	2
MMESO/HEMA30	15.81 ± 0.13	259.2 ± 7.3	8.99 ± 0.60	3	H	2
MMERSO/HEMA30	10.12 ± 0.55	186.7 ± 6.9	14.56 ± 1.11	2	2B	2
MMEWSO/HEMA30	2.41 ± 0.29	11.8 ± 0.6	19.58 ± 1.36	2	4B	2

<sup>a</sup> Tensile strength. <sup>b</sup> Tensile modulus. <sup>c</sup> Elongation at the break. <sup>d</sup> Adhesion. <sup>e</sup> Pencil hardness. <sup>f</sup> Flexibility.

### 3.4.4. Coating Properties

The coating properties of the cured EA-like materials were analyzed, and the related results are listed in Table 4. Firstly, the pure MMESO film exhibited better adhesion and pencil hardness than the neat AESO film, which is most likely because of the higher  $\nu_e$ . The neat MMERSO and MMEWSO films possessed equal adhesion, pencil hardness, and flexibility as those of neat AESO film. However, compared to the AESO/HEMA30 materials, the UV-cured EA/HEMA materials demonstrated lower pencil hardness, which is possibly ascribed to the larger drop of  $\nu_e$ . Secondly, as the C=C functionality rises, the adhesion and pencil hardness of the neat EA-like films increased slightly, while only the pencil hardness of the EA/HEMA films increased apparently. The increase in hardness can also be attributed to the improvement of  $\nu_e$ . Finally, a significant improvement of adhesion and pencil hardness values was observed when incorporating 30% of HEMA diluent, indicating that the addition of HEMA diluent had a positive impact on the coating performances.

### 3.5. UV-Curing Kinetics of the EA-Like Resins

Photopolymerization behaviors of the EA-like resins were measured by the Real-time Fourier Transform Infrared Spectroscopy (RT-IR) technique. The real-time C=C conversion of liquid resin was analyzed by monitoring the  $810\text{ cm}^{-1}$  peak intensity [43,44], as shown in Figure 6. Obviously, the C=C functional groups of both EA and EA/HEMA materials were rapidly polymerized and reached the highest rates of C=C conversion ( $da/dt$ ) in less than 50 s, and the C=C conversions were all above 60%

after 150 s. Therefore, we can conclude that they have excellent copolymerization reactivity. As the C=C functionality increases, the final C=C conversion of the pure EA materials improved from 74.7% to 85.0%. For the EA/HEMA materials, the final C=C conversion improved from 77.1% to 92.9%. When incorporating 30% of HEMA diluent into the EA prepolymers, the final C=C conversions were also improved, which is probably caused by the good diluting effect of HEMA [21,22]. Specially, the pure MMESO resin demonstrated a lower final C=C conversion compared to the AESO resins, which is mainly caused by the effect of a steric hindrance for both maleic and allylic C=C groups in the oil-based EA systems. However, due to the higher C=C functionality of the MMESO oligomer compared to that of the AESO, the resulting MMESO material still indicated higher cross-link density when cross-linking [30]. Similar results were demonstrated when comparing the MMESO/HEMA30 materials with the AESO/HEMA30 materials.

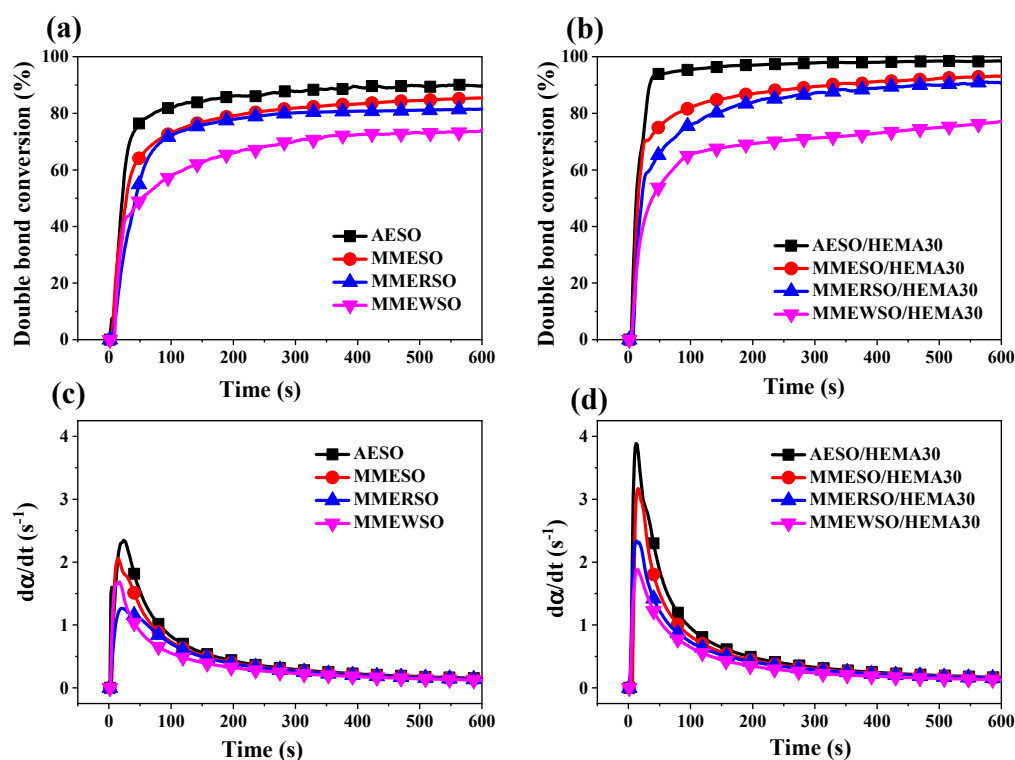


**Figure 6.** Double bonds conversion rates (a,b) and polymerization rates (c,d) of the UV-cured EA-like materials.

#### 4. Conclusions

In this study, we firstly synthesized a series of novel oil-based EA-like prepolymers with different C=C functionality through the modification of epoxidized plant oils with MAAMA, which is a new unsaturated carboxyl acid compound with two active C=C groups and a methyl group. Both the UV-cured pure MMESO and MMESO/HEMA materials showed much better stiffness and heat resistance such as  $E'_{25}$ ,  $T_g$ ,  $\sigma$ , and  $E$  than the corresponding AESO materials. Both the UV-cured pure MMERSO and MMERSO/HEMA materials also exhibited clearly better stiffness and heat resistance than the corresponding AESO materials, although ERSO had an obvious lower epoxy value than AESO. These results indicated that the MAAMA modification of epoxidized plant oils was much more effective than the AA modification for preparing high-performance oil-based epoxy acrylate resins. In addition, we investigated two important effects, the C=C functionality of such EA-like prepolymers and the incorporation of HEMA diluent, on the ultimate properties and UV-curing behaviors of the resulting UV-cured materials and established the structure–property relationships successfully for the obtained EA-like materials. By the increase of C=C functionality of the EA prepolymers or the

incorporation of HEMA diluent, most of the important properties including  $E'_{25}$ ,  $T_g$ ,  $T_5$ ,  $T_p$ ,  $\sigma$ ,  $E$ , and hardness of coating increased generally for both the pure EA and EA/HEMA resins. The growths mainly result from the rise of  $\nu_e$  or the incorporation of methyl steric hindrance or both. In general, this study could not only provide several high-performance UV-curable oil-based EA resins which can be applied in the fields of coatings such as wood coatings but also offer substantial fundamental research for tuning their properties and the UV-curing process for the coating application.

**Supplementary Materials:** The following are available online at <http://www.mdpi.com/2073-4360/12/9/2165/s1>, Figure S1: Acid values of MAAMA, Figure S2: FT-IR spectra of (a) ERSO, (b) MMERSO, (c) EWSO, and (d) MMEWSO, Figure S3:  $^1\text{H}$  NMR spectrum of (a) ERSO, (b) MMERSO, (c) EWSO, and (d) MMEWSO, Figure S4:  $^1\text{H}$  NMR spectrum of MAAMA, Figure S5:  $^1\text{H}$  NMR spectrum of ESO, Figure S6:  $^1\text{H}$  NMR spectrum of ERSO, Figure S7:  $^1\text{H}$  NMR spectrum of EWSO, Figure S8:  $^1\text{H}$  NMR spectrum of MMESO, Figure S9:  $^1\text{H}$  NMR spectrum of MMERSO, Figure S10:  $^1\text{H}$  NMR spectrum of MMEWSO, Figure S11:  $^1\text{H}$  NMR spectrum of AESO, Equation (S1): Determining the grafted C=C functionality for AESO.

**Author Contributions:** Supervision and Writing—Review and Editing, J.T. and C.L.; Writing—Original Draft, J.Z.; Validation and Formal analysis, J.L., J.H. and F.Z.; Data Curation, Y.H.; Characterization, H.M., Y.C. and T.H.; Conceptualization, Visualization, R.A.; Project administration and Funding acquisition, C.L., and Y.Z. All authors have read and agreed to the published version of the manuscript.

**Funding:** This research was funded by the National Natural Science Foundation of China (31822009 and 31770615), the Fundamental Research Funds of CAF (CAFYBB2020QA005 and CAFYBB2017QB006), and the Natural Science Foundation of the Higher Education Institutions of Jiangsu Province (17KJB140017).

**Acknowledgments:** This paper would not have been possible without the consistent and valuable reference materials that I received from my supervisor, whose insightful guidance and enthusiastic encouragement in the course of my shaping this thesis definitely gain my deepest gratitude.

**Conflicts of Interest:** The authors declare no competing financial interest.

## References

1. Zovi, O.; Lecamp, L.; Loutelier-Bourhis, C.; Lange, C.M.; Bunel, C. A solventless synthesis process of new UV-curable materials based on linseed oil. *Green Chem.* **2001**, *13*, 1014–1022. [[CrossRef](#)]
2. Ma, S.; Jiang, Y.; Liu, X.; Fan, L.; Zhu, J. Bio-based tetrafunctional crosslink agent from gallic acid and its enhanced soybean oil-based UV-cured coatings with high performance. *RSC Adv.* **2014**, *4*, 23036–23042. [[CrossRef](#)]
3. Wang, Q.; Chen, G.; Cui, Y.; Tian, J.; He, M.; Yang, J.-W. Castor Oil Based Biothiol as a Highly Stable and Self-Initiated Oligomer for Photoinitiator-Free UV Coatings. *ACS Sustain. Chem. Eng.* **2016**, *5*, 376–381. [[CrossRef](#)]
4. Zhang, W.; Ma, H.; Han, X.; Zhou, Z.; Xu, W.; Ren, F. Synthesis and properties of unsaturated modified linoleate for fast UV-curable coatings. *Energ. Source Part A* **2019**, 1–10. [[CrossRef](#)]
5. Shen, L.; Pan, Y.; Fu, H. Fabrication of UV curable coating for super hydrophobic cotton fabrics. *Polym. Eng. Sci.* **2019**, *59*. [[CrossRef](#)]
6. Ang, D.T.C.; Gan, S.N. Novel approach to convert non-self drying palm stearin alkyds into environmental friendly UV curable resins. *Prog. Org. Coat.* **2012**, *73*, 409–414. [[CrossRef](#)]
7. Dai, J.; Liu, X.; Ma, S.; Wang, J.; Shen, X.; You, S.; Zhu, J. Soybean oil-based UV-curable coatings strengthened by crosslink agent derived from itaconic acid together with 2-hydroxyethyl methacrylate phosphate. *Prog. Org. Coat.* **2016**, *97*, 210–215. [[CrossRef](#)]
8. Huang, Y.; Ye, G.; Yang, J. Synthesis and properties of UV-curable acrylate functionalized tung oil based resins via Diels–Alder reaction. *Prog. Org. Coat.* **2015**, *78*, 28–34. [[CrossRef](#)]
9. Patil, D.M.; Phalak, G.A.; Mhakse, S.T. Boron-containing UV-curable oligomer-based linseed oil as flame-retardant coatings: Synthesis and characterization. *Iran. Polym. J.* **2018**, *27*, 795–806. [[CrossRef](#)]
10. Biermann, U.; Bornscheuer, U.; Meier, M.A.; Metzger, J.O.; Schafer, H.J. Oils and fats as renewable raw materials in chemistry. *Angew Chem. Int. Ed. Engl.* **2011**, *50*, 3854–3871. [[CrossRef](#)]
11. Ahn, B.K.; Sung, J.; Kim, N.; Kraft, S.; Sun, X.S. UV-curable pressure-sensitive adhesives derived from functionalized soybean oils and rosin ester. *Polym. Int.* **2013**, *62*, 1293–1301. [[CrossRef](#)]

12. Sharmin, E.; Zafar, F.; Akram, D.; Alam, M.; Ahmad, S. Recent advances in vegetable oils based environment friendly coatings: A review. *Ind. Crop. Prod.* **2015**, *76*, 215–229. [[CrossRef](#)]
13. Fertier, L.; Koleilat, H.; Stemmelen, M.; Giani, O.; Joly-Duhamel, C.; Lapinte, V.; Robin, J.-J. The use of renewable feedstock in UV-curable materials—A new age for polymers and green chemistry. *Prog. Polym. Sci.* **2013**, *38*, 932–962. [[CrossRef](#)]
14. Huang, Y.; Pang, L.; Wang, H.; Zhong, R.; Zeng, Z.; Yang, J. Synthesis and properties of UV-curable tung oil based resins via modification of Diels—Alder reaction, nonisocyanate polyurethane and acrylates. *Prog. Org. Coat.* **2013**, *76*, 654–661. [[CrossRef](#)]
15. Rengasamy, S.; Mannari, V. Development of soy-based UV-curable acrylate oligomers and study of their film properties. *Prog. Org. Coat.* **2013**, *76*, 78–85. [[CrossRef](#)]
16. Wu, J.; Zhang, T.; Ma, G.; Li, P.; Ling, L.; Wang, B. Synthesis of a tung oil-rosin adduct via the diels-alder reaction: Its reaction mechanism and properties in an ultraviolet-curable adhesive. *J. Appl. Polym. Sci.* **2013**, *130*. [[CrossRef](#)]
17. Li, K.; Shen, Y.; Fei, G.; Wang, H.; Li, J. Preparation and properties of castor oil/pentaerythritol triacrylate-based UV curable waterborne polyurethane acrylate. *Prog. Org. Coat.* **2015**, *78*, 146–154. [[CrossRef](#)]
18. Liu, J.; Liu, R.; Zhang, X.; Li, Z.; Tang, H.; Liu, X. Preparation and properties of UV-curable multi-arms cardanol-based acrylates. *Prog. Org. Coat.* **2016**, *90*, 126–131. [[CrossRef](#)]
19. Liang, B.; Li, R.; Zhang, C.; Yang, Z.; Yuan, T. Synthesis and characterization of a novel tri-functional bio-based methacrylate prepolymer from castor oil and its application in UV-curable coatings. *Ind. Crop. Prod.* **2019**, *135*, 170–178. [[CrossRef](#)]
20. Chen, Z.; Wu, J.F.; Fernando, S.; Jagodzinski, K. Soy-based, high biorenewable content UV curable coatings. *Prog. Org. Coat.* **2011**, *71*, 98–109. [[CrossRef](#)]
21. Wu, J.F.; Fernando, S.; Jagodzinski, K.; Weerasinghe, D.; Chen, Z. Effect of hyperbranched acrylates on UV-curable soy-based biorenewable coatings. *Polym. Int.* **2011**, *60*, 571–577. [[CrossRef](#)]
22. Li, P.; Ma, S.; Dai, J.; Liu, X.; Jiang, Y.; Wang, S.; Wei, J.; Chen, J.; Zhu, J. Itaconic Acid as a Green Alternative to Acrylic Acid for Producing a Soybean Oil-Based Thermoset: Synthesis and Properties. *ACS Sustain. Chem. Eng.* **2016**, *5*, 1228–1236. [[CrossRef](#)]
23. Kahraman, M.V.; Bayramoğlu, G.; Boztoprak, Y.; Güngör, A.; Kayaman-Apohan, N. Synthesis of fluorinated/methacrylated epoxy based oligomers and investigation of its performance in the UV curable hybrid coatings. *Prog. Org. Coat.* **2009**, *66*, 52–58. [[CrossRef](#)]
24. Xiao, M.; He, Y.; Nie, J. Novel Bisphenol A Epoxide–Acrylate Hybrid Oligomer and Its Photopolymerization. *Des. Monomers Polym.* **2012**, *11*, 383–394. [[CrossRef](#)]
25. Öztürk, C.; Küsefoğlu, S.H. Polymerization of epoxidized soybean oil with maleinized soybean oil and maleic anhydride grafted polypropylene mixtures. *J. Appl. Polym. Sci.* **2010**, *118*, 3311–3317. [[CrossRef](#)]
26. Li, Y.; Sun, X.S. Di-Hydroxylated Soybean Oil Polyols with Varied Hydroxyl Values and Their Influence on UV-Curable Pressure-Sensitive Adhesives. *J. Am. Oil Chem. Soc.* **2014**, *91*, 1425–1432. [[CrossRef](#)]
27. Wu, Y.; Li, K. Acrylated epoxidized soybean oil as a styrene replacement in a dicyclopentadiene-modified unsaturated polyester resin. *J. Appl. Polym. Sci.* **2018**, *135*. [[CrossRef](#)]
28. Liu, H.; Lu, W.; Liu, S. Development of acrylated soybean oil-based UV-curable coatings with high impact strength from low viscosity oligomer. *J. Appl. Polym. Sci.* **2018**, *135*. [[CrossRef](#)]
29. Wu, Y.; Li, K. Replacement of styrene with acrylated epoxidized soybean oil in an unsaturated polyester resin from propylene glycol and maleic anhydride. *J. Appl. Polym. Sci.* **2017**, *134*. [[CrossRef](#)]
30. Wu, Q.; Hu, Y.; Tang, J.; Zhang, J.; Wang, C.; Shang, Q.; Feng, G.; Liu, C.; Zhou, Y.; Lei, W. High-Performance Soybean-Oil-Based Epoxy Acrylate Resins: “Green” Synthesis and Application in UV-Curable Coatings. *ACS Sustain. Chem. Eng.* **2018**, *6*, 8340–8349. [[CrossRef](#)]
31. Bakare, I.O.; Pavithran, C.; Okieimen, F.E.; Pillai, C.K.S. Polyesters from renewable resources: Preparation and characterization. *J. Appl. Polym. Sci.* **2006**, *100*, 3748–3755. [[CrossRef](#)]
32. Satyanarayana, M.; Muraleedharan, C. Comparative Studies of Biodiesel Production from Rubber Seed Oil, Coconut Oil, and Palm Oil Including Thermogravimetric Analysis. *Energ. Source Part A* **2011**, *33*, 925–937. [[CrossRef](#)]
33. Liu, Q.; Lei, X.; Cao, Z.; Zhang, J.; Kuang, T.; Liu, G.; Fang, Y.; Qian, K.; Fu, J.; Du, H.; et al. Protective effect of oil from *Cornus wilsoniana* fruits against carbon tetrachloride-induced hepatic fibrosis in mice. *Food Nutr. Res.* **2020**, *64*. [[CrossRef](#)]

34. Onoji, S.E.; Iyuke, S.E.; Igbafe, A.I.; Nkazi, D.B. Rubber seed oil: A potential renewable source of biodiesel for sustainable development in sub-Saharan Africa. *Energ. Convers. Manag.* **2016**, *110*, 125–134. [[CrossRef](#)]
35. Aigbodion, A.I.; Okieimen, F.E.; Obaze, E.O.; Bakare, I.O. Utilisation of maleinized rubber seed oil and its alkyd resin as binders in water-borne coatings. *Prog. Org. Coat.* **2003**, *46*, 28–31. [[CrossRef](#)]
36. Aigbodion, A.I.; Pillai, C.K.S. Preparation, analysis and applications of rubber seed oil and its derivatives in surface coatings. *Prog. Org. Coat.* **2000**, *38*, 187–192. [[CrossRef](#)]
37. Ikhuria, E.U.; Maliki, M.; Okieimen, F.E.; Aigbodion, A.I.; Obaze, E.O.; Bakare, I.O. Synthesis and characterisation of chlorinated rubber seed oil alkyd resins. *Prog. Org. Coat.* **2007**, *52*, 134–137. [[CrossRef](#)]
38. Chen, J.; Li, X.; Wang, Y.; Huang, J.; Li, K.; Nie, X.; Jiang, J. Epoxidized dimeric acid methyl ester derived from rubber seed oil and its application as secondary plasticizer. *J. Appl. Polym. Sci.* **2016**, *133*. [[CrossRef](#)]
39. Chaikul, P.; Lourith, N.; Kanlayavattanakul, M. Antimelanogenesis and cellular antioxidant activities of rubber (*Hevea brasiliensis*) seed oil for cosmetics. *Ind. Crop. Prod.* **2017**, *108*, 56–62. [[CrossRef](#)]
40. Liu, C.; Dai, Y.; Hu, Y.; Shang, Q.; Feng, G.; Zhou, J.; Zhou, Y. Highly Functional Unsaturated Ester Macromonomer Derived from Soybean Oil: Synthesis and Copolymerization with Styrene. *ACS Sustain. Chem. Eng.* **2016**, *4*, 4208–4216. [[CrossRef](#)]
41. Liang, B.; Zhao, J.; Li, G.; Huang, Y.; Yang, Z.; Yuan, T. Facile synthesis and characterization of novel multi-functional bio-based acrylate prepolymers derived from tung oil and its application in UV-curable coatings. *Ind. Crop. Prod.* **2019**, *138*. [[CrossRef](#)]
42. Liu, C.; Wang, C.; Hu, Y.; Zhang, F.; Shang, Q.; Lei, W.; Zhou, Y.; Cai, Z. Castor oil-based polyfunctional acrylate monomers: Synthesis and utilization in UV-curable materials. *Prog. Org. Coat.* **2018**, *121*, 236–246. [[CrossRef](#)]
43. Liu, R.; Zhang, X.; Zhu, J.; Liu, X.; Wang, Z.; Yan, J. UV-Curable Coatings from Multiarmed Cardanol-Based Acrylate Oligomers. *ACS Sustain. Chem. Eng.* **2015**, *3*, 1313–1320. [[CrossRef](#)]
44. Liu, R.; Zhu, G.; Li, Z.; Liu, X.; Chen, Z.; Ariyasivam, S. Cardanol-based oligomers with “hard core, flexible shell” structures: From synthesis to UV curing applications. *Green Chem.* **2015**, *17*, 3319–3325. [[CrossRef](#)]
45. Liang, B.; Kuang, S.; Huang, J.; Man, L.; Yang, Z.; Yuan, T. Synthesis and characterization of novel renewable tung oil-based UV-curable active monomers and bio-based copolymers. *Prog. Org. Coat.* **2019**, *129*, 116–124. [[CrossRef](#)]
46. Huang, J.; Yuan, T.; Ye, X.; Man, L.; Zhou, C.; Hu, Y.; Zhang, C.; Yang, Z. Study on the UV curing behavior of tung oil: Mechanism, curing activity and film-forming property. *Ind. Crop. Prod.* **2018**, *112*, 61–69. [[CrossRef](#)]
47. Phalak, G.; Patil, D.; Vignesh, V.; Mhaske, S. Development of tri-functional biobased reactive diluent from ricinoleic acid for UV curable coating application. *Ind. Crop. Prod.* **2018**, *119*, 9–21. [[CrossRef](#)]
48. Kolanthai, E.; Sarkar, K.; Meka, S.R.K.; Madras, G.; Chatterjee, K. Copolyesters from Soybean Oil for Use as Resorbable Biomaterials. *ACS Sustain. Chem. Eng.* **2015**, *3*, 880–891. [[CrossRef](#)]
49. Caillol, S.; Desroches, M.; Boutevin, G.; Loubat, C.; Auvergne, R.; Boutevin, B. Synthesis of new polyester polyols from epoxidized vegetable oils and biobased acids. *Eur. J. Lipid Sci. Tech.* **2012**, *114*, 1447–1459. [[CrossRef](#)]
50. Yang, X.; Li, S.; Xia, J.; Song, J.; Huang, K.; Li, M. Novel renewable resource-based UV-curable copolymers derived from myrcene and tung oil: Preparation, characterization and properties. *Ind. Crop. Prod.* **2015**, *63*, 17–25. [[CrossRef](#)]
51. Duan, H.; Dong, W.; Wang, X.; Tao, X.; Ma, H. UV-curable polyurethane acrylate resin containing multiple active terminal groups for enhanced mechanical properties. *J. Appl. Polym. Sci.* **2019**, *136*. [[CrossRef](#)]

